

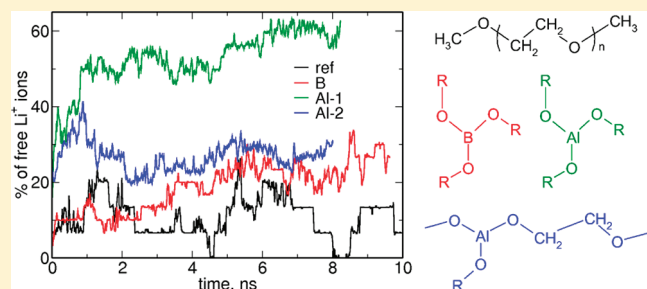
Molecular Dynamics Study on the Effect of Lewis Acid Centers in Poly(ethylene oxide)/LiClO₄ Polymer Electrolyte

Andrzej Eilmes* and Piotr Kubisiak

Faculty of Chemistry, Jagiellonian University, Ingardena 3, 30-060 Kraków, Poland

Supporting Information

ABSTRACT: Molecular dynamics simulations employing a polarizable force field have been performed for the model poly(ethylene oxide)/LiClO₄ electrolytes with boron or aluminum centers. Influence of Lewis acid centers on radial distribution functions, coordination numbers, percentage of free cations, diffusion coefficients and conductivity has been investigated. Results confirm the effect of acid centers on ion complexation and show that the properties of the electrolyte result from interplay of different interactions.



1. INTRODUCTION

Technological applications of solid polymer electrolytes, such as lithium batteries, fuel cells, solid-state electrochemical devices, displays, and sensors, stimulate continuing interest in their research. An electrolyte of such a type consists of an inorganic salt dissolved in a polymer; a common example is a poly(ethylene oxide) (PEO) matrix loaded with lithium salt (e.g., lithium perchlorate).

Ion-transport properties of polymer electrolytes are therefore closely related to the strength of ion–ion and ion–polymer interactions. Modification of these factors provides a way to optimize parameters of the electrolyte. For practical applications it is usually desirable to promote salt dissociation and to increase cation transference numbers.

It has been suggested that increased cation conductivity may be achieved by enriching the electrolyte with Lewis acid centers, which act as complexing sites for anions, reducing therefore their mobility and facilitating ion-pair breaking. Boron^{1–5} or aluminum^{6,7} atoms were used as Lewis acids in experiments, either incorporated directly into polymer backbone^{1–3} or added in small plasticizer molecules.^{4–7}

Several theoretical works were devoted to study Li⁺–polymer interactions in PEO by means of quantum-chemical methods.^{8–14} Molecular dynamics (MD) simulations were applied to analyze ion transport in solid electrolytes based on PEO.^{15–19} Likewise, quantum-chemical methodology was used to estimate the possibility of anion binding to boron^{5,20–22} or aluminum²¹ centers; quantum-chemical calculations employing ab initio MD were also performed for small systems of lithium aluminate salts.²³ However, no classical MD study on the effect of Lewis acid centers in polymer electrolytes has been presented. Although quantum-chemical computations yield information about optimal structures and interaction energies in small model systems, MD simulations are needed to gain some insight about dynamics and to obtain parameters related to ion-transport in the electrolyte.

In this work we aim to fill this gap, modeling the PEO/LiClO₄ doped with boron or aluminum acid centers. Although perchlorate salts are not used in practical applications, PEO loaded with lithium perchlorate is a classical example of polymer electrolyte, investigated in numerous experimental and theoretical works, and therefore constitutes a good model system. In following sections we present parametrization of the polarizable force-field and then details of the MD simulations. Next we analyze collected MD trajectories focusing on ion coordination numbers and ion transport properties.

2. FORCE FIELD PARAMETRIZATION

2.1. Force Field Atom Types. Several works employed MD simulations to study lithium salts dissolved in poly(ethylene oxide),^{15–17,19} therefore many force-field parametrizations for unmodified PEO are already available in the literature. However, to the best of our knowledge, such studies have not been performed for systems with Lewis acid centers and appropriate parametrization has not been constructed. Therefore, we had to start our study with development of force-field parametrization for boron and aluminum centers in PEO-based electrolytes.

In Figure 1 we display structures of molecules for which our parametrization is developed. We distinguished between two types of carbon and hydrogen atoms, from backbone CH₂ and terminal CH₃ groups, respectively. Three types of oxygen atoms in polymer molecules were introduced: oxygen atoms from PEO repeat units and oxygen atoms bonded directly to boron or aluminum atom. The first type of oxygen atom was used both for atoms from polymer backbone and for atoms from side chains in

Received: August 29, 2011

Revised: November 7, 2011

Published: November 10, 2011

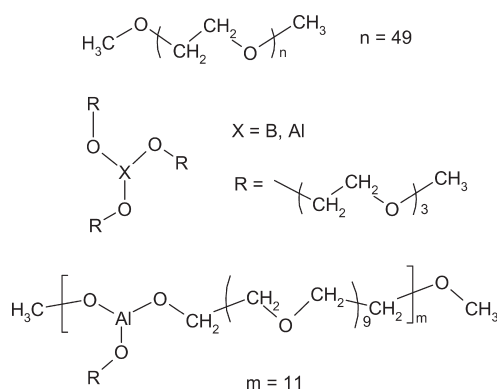


Figure 1. Chemical formulas of investigated systems. From top to bottom: PEO chain, plasticizer molecules with B or Al atoms, and PEO-like chain with aluminum centers.

small molecules with acid centers. The fourth type of oxygen atom (O_{perch}) was used for oxygen atoms from the perchlorate anion.

2.2. Initial Parametrization. Gaussian 09 rev. A02²⁴ was used in all quantum-chemical calculations used in determination of force-field parameters.

Parameters of bonded interactions and of Lennard-Jones potential for the $-O-CH_2-CH_2-$ repeat units and terminal CH_3 groups were transferred from the AMBER force field for organic compounds.²⁵

Parameters responsible for the description of bonds, angles and dihedrals at the boron center were adopted from the FF for alkyl boronates.²⁶ In ref 26 parametrization of van der Waals interactions was based on MM2 force field using Buckingham potential.²⁷ In our work we used Lennard-Jones potential²⁸ for all atoms and therefore we needed to adjust appropriately corresponding van der Waals parameters. Values of r_{min} and ϵ for B and adjacent O atoms were obtained from the fits of the Lennard-Jones energy curves to the values of Buckingham potential calculated for parameters from ref 26 (plots of the fitted potential curves are presented in the Supporting Information). Bonded-interactions parameters and Lennard-Jones-type van der Waals parameters at aluminum center were based on the universal force field (UFF).²⁹

Lennard-Jones potential parameters for the lithium cation were adopted from the AMBER force field.²⁵ In the case of the perchlorate anion, values taken from a recent MD study³⁰ were used. Bond lengths and partial charges for ClO_4^- were determined from quantum-chemical calculations (MP2/aug-cc-pVDZ); charges were obtained from the Merz–Kollman fit to electrostatic potential. Appropriate force constants for bonds and valence angles were calculated by fitting the energy curves calculated at the MP2/aug-cc-pVDZ level for structures with one or four bonds stretched or with altered values of valence angles.

Assigning partial charges to the atoms from PEO chains and molecules with acid centers requires imposing constraints to ensure electroneutrality of molecules. Accordingly, the net zero charge has been ascribed to the PEO repeat units ($O-CH_2-CH_2$ groups) and to the CH_3-O-CH_3 groups. These conditions allow for construction of CH_3 -terminated neutral polymer chains of any length. Likewise, we introduced additional condition that the total charge of three CH_3 groups balances the net charge of $Al-O_3$ or $B-O_3$ group (acid center with three adjacent

Table 1. Comparison between Values of Li^+ Binding Energies to Oligoglymes Calculated Quantum-Chemically (MP2/aug-cc-pVDZ) and Obtained from the Final Force-Field Parameterization

structure ^a	Li^+ coord. number	E_{QC} [kcal/mol]	E_{FF} [kcal/mol]
1a	1	−40.4	−38.1
1b	2	−64.4	−58.0
1c	3	−80.1	−72.9
1d	4	−97.0	−84.0
1e	5	−110.4	−93.6
1f	6	−124.7	−95.0
1g	6	−129.1	−108.9

^a Labels as in ref 31, from which the optimized geometries were taken.

oxygen atoms) enforcing neutrality of plasticizer molecules with B or Al atoms and of PEO chains with Lewis acid centers linked to PEO-like side chains.

Initial values of partial charges on PEO repeat units originated from ref 16, they were, however, subsequently modified to better reproduce the interactions between Li^+ and model oligoglyme molecules (cf. section 2.3). Charges for B, Al, and O atoms at acid centers were determined using the Merz–Kollman method to fit partial charges to the electrostatic potential calculated at the B3LYP/aug-cc-pVDZ level for $B(OCH_3)_3$ and $Al(OCH_3)_3$ molecules; obtained values were then rescaled to satisfy above-described constraints. This procedure yielded 1.16e and −0.56e for B and neighboring O atom, respectively, or 1.64e for Al atom and −0.72e for oxygen atom directly bonded to Al center.

2.3. Polarizable Force Field. Initial parametrization described in the previous subsection was subsequently improved by addition of atomic polarizabilities and modification of selected nonbonded parameters to better match quantum-chemically calculated energies.

Initial values of polarizabilities of carbon, oxygen and hydrogen atoms from PEO chains were adopted from ref 16. These values as well as partial atomic charges and Lennard-Jones potential parameters for selected atom pairs ($O-Li$, $C_{(CH_2)}-O_{\text{perch}}$ and $H-O_{\text{perch}}$) were adjusted in the following procedure. We calculated at the MP2/aug-cc-pVDZ level complexation energies of model oligoglyme molecules with Li^+ ion (geometries of optimized structures were taken from ref.³¹) and compared these values to the energies based on force-field parametrization. Then we sought the set of FF parameters which provided the best fit between quantum-chemical and FF-based values. As an additional test of modified parameters we also checked how their changes affected the geometries of complexes, mainly Li^+-O distances. In Table 1 we compare complexation energies obtained from quantum-chemical calculations and from our final set of force field parameters. It is clearly visible that FF energies underestimate the strength of Li^+-O interactions and that this effect increases with the increase in the number of oxygen atoms coordinating the lithium cation. For CN = 1 the difference is relatively small (2 kcal/mol) but for CN = 4 amounts to 13 kcal/mol and for CN = 6 increases to approximately 20–30 kcal/mol. None of the investigated sets of parameters was able to reproduce the complexation energy in the whole range of coordination numbers. For some sets we achieved improvement for larger coordination numbers but at the cost of increasing discrepancies for smaller CNs. In addition, in such instances we observed that structures of complexes changed so that Li^+-O distances were too

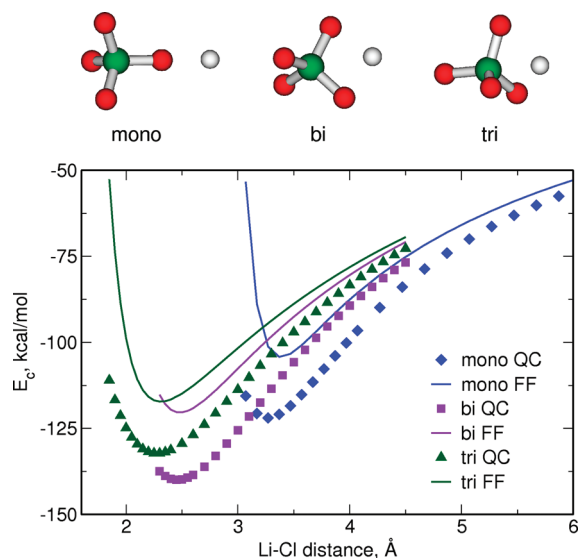


Figure 2. Binding energies for $\text{Li}^+ - \text{ClO}_4^-$ ion pair in mono-, bi-, and tridentate configuration obtained from quantum-chemical (MP2/aug-cc-pVDZ) calculations and from the final force-field parametrization.

small in comparison with quantum-chemical data. Eventually, the set of parameters presented in Table 1 was chosen as the best compromise between reproduction of quantum-chemically determined energies for different coordination numbers and geometries matching the quantum-chemical data.

Parameters for the $\text{Li}^+ - \text{ClO}_4^-$ ion pair were modified in an analogous manner. We altered van der Waals parameters for $\text{Li}-\text{O}_{\text{perch}}$ and $\text{Li}-\text{Cl}$ interactions to fit the binding energies obtained from quantum-chemical MP2/aug-cc-pVDZ calculations for three paths of Li^+ approaching the anion in mono-, bi-, and tridentate configuration. In Figure S2 in the Supporting Information we display energies calculated using initial set of parameters and the best fit reproducing the MP2 data. However, in MD simulations we used different values. As mentioned in preceding paragraph, our FF parametrization underestimates Li^+ -oligoglyme complexation energies. To compensate this effect we decided to shift the $\text{Li}^+ - \text{ClO}_4^-$ binding energies by approximately the same value, adjusting the van der Waals parameters. Simultaneously we modified these parameters to match the position of energy minima ($\text{Li}^+ - \text{O}$ distances) for bi- and tridentate configuration to quantum chemical data. Final energy curves are presented in Figure 2.

Last part of force field adjustment was the modification of selected nonbonded parameters at the Lewis acid centers (boron or aluminum atoms). Values of atomic polarizabilities of the boron atom and the adjacent oxygen atoms were estimated as a difference between the calculated polarizability of the whole $\text{B}(\text{OCH}_3)_3$ molecule and the sum of polarizabilities of $\text{O}-\text{CH}_3$ groups³² (results of B3LYP/aug-cc-pVDZ level were rescaled to the values obtained for Sadlej basis set). Polarizability of the aluminum atom was estimated in similar manner.

Modifications were applied to the van der Waals parameters describing interactions between acid centers and the oxygen or chlorine atoms from the perchlorate anion to fit the energies obtained from the quantum-chemical MP2/aug-cc-pVDZ calculations for perchlorate anion approaching the Lewis acid center in $\text{B}(\text{OCH}_3)_3$ or $\text{Al}(\text{OCH}_3)_3$ molecules with one of $\text{Cl}-\text{O}$ bonds

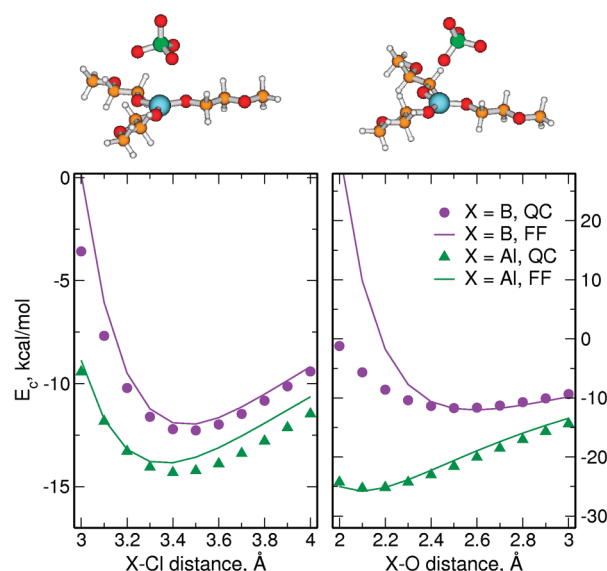


Figure 3. Binding energies for perchlorate anion approaching the acid center (B or Al atom) obtained from MP2/aug-cc-pVDZ calculations and from the final force-field parametrization.

pointing toward or outward the center. The best fit is displayed in Figure 3. As readily seen, the agreement between quantum-chemical and FF energies is very good, especially near the minimum of the potential energy.

All parameters of the polarizable force field developed in this work are collected in the Supporting Information.

3. MD SIMULATIONS

3.1. Model Systems and Simulation Details. Initial geometries of model systems were constructed using Polymer Builder and Amorphous Cell from Materials Studio.³³ Reference electrolyte, without Lewis acid centers, consisted of 6 CH_3 -terminated PEO chains, 50 repeat units each, and 15 $\text{Li}^+ - \text{ClO}_4^-$ pairs. This salt concentration corresponds to a $[\text{Li}^+]/[\text{O}_{\text{PEO}}]$ ratio equal 1:20. Electrolytes with acid centers introduced in plasticizer molecules contained 4×50 units PEO chains, $44\text{X}[(\text{OCH}_2\text{CH}_2)_3\text{OCH}_3]_3$ molecules ($\text{X} = \text{B}$ or Al) and 30 ion pairs. Although the number of polymer chains was smaller, side chains of plasticizer molecules were short PEO oligomers; therefore, the total number of PEO-like oxygen atoms in the system increased. The $[\text{Li}^+]/[\text{O}_{\text{PEO}}]$ ratio in the plasticized electrolyte was about 1:24. These values correspond to salt and boron center concentrations used in experimental studies.^{2,7} Alternatively, Al-containing electrolyte was constructed with aluminum atoms incorporated into polymer backbone. This system contained four PEO chains with 11 Al-centers each and 30 $\text{Li}^+ - \text{ClO}_4^-$ ion pairs, therefore the total number of Al atoms and ions was the same as in the electrolyte with aluminate plasticizer. Initial density of systems was 1.18 and 1.13 g/cm^3 for reference electrolyte and electrolytes with acid centers, respectively. Lithium and perchlorate ions in initial structures were introduced as ion pairs to observe dissociation of ion aggregates in the course of simulation. Hereafter the systems will be referred to as “REF” (reference electrolyte without acid centers), “B” (electrolyte with boron atoms) and “Al” and “Al-2”

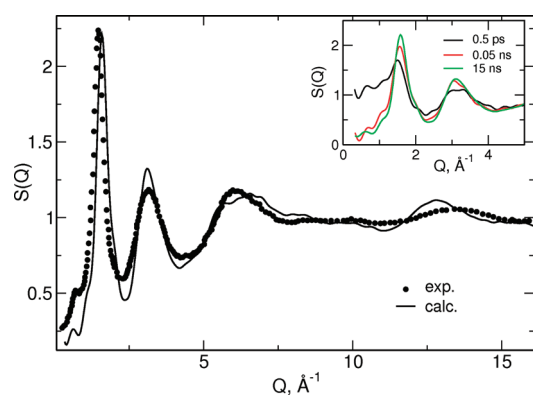


Figure 4. Static structure factors calculated for the last 2 ns of the REF trajectory (with H atoms substituted by D). Experimental data from ref 36. Inset: time evolution of calculated structure factor.

Table 2. Composition of Investigated Model Electrolytes

system	$[\text{Li}^+]/[\text{O}_{\text{pol}}]$	$[\text{X}]/[\text{O}_{\text{pol}}]$ $\text{X} = \text{B, Al}$	$n(\text{LiClO}_4)$	$c(\text{LiClO}_4)$ [mol/ dm^3]	ρ^a [g/cm^3]
REF	1:20		15	1.21	1.185
B	1:24.3	1:16.5	30	1.01	1.14
Al	1:24.3	1:16.5	30	1.00	1.16
Al-2	1:22	1:15	30	1.14	1.20

^a density of the system averaged over 5 ps of MD trajectory.

(electrolytes with aluminum atoms added in plasticizer or incorporated into polymer, respectively).

Tinker 5.0 was used for MD simulations.³⁴ All simulations were performed in NPT ensemble at $T = 360$ K and $p = 1$ atm using the Berendsen thermostat and barostat. Default Tinker values of 0.1 and 2.0 ps were used as the coupling time for temperature and pressure bath, respectively. Beeman algorithm with time step of 1 fs was used to integrate the equations of motion. Ewald summation was used to treat electrostatic interactions. Induced dipoles were calculated iteratively assuming mutual interactions between polarizable units to achieve self-convergence; the Thole scheme of short-range polarization damping³⁵ was applied.

Individual frames from MD simulations were saved for further analysis in 0.5 ps intervals. Total length of accumulated trajectories ranged from 8 ns for Al-2 to 15 ns for REF electrolyte.

3.2. Results and Discussion. *Structure of Electrolytes.* After initial relaxation of the electrolyte during about 2 ns, density of the systems stabilized. Average density of REF electrolyte was about $1.185 \text{ g}/\text{cm}^3$, close to the value for the initial structure. Densities of electrolytes with plasticizer molecules were remarkably lower and amounted to 1.14 and $1.16 \text{ g}/\text{cm}^3$ for B and Al electrolytes, respectively. On the other hand, density of the Al-2 system was $1.20 \text{ g}/\text{cm}^3$ and exceeded that of the reference electrolyte. A plot of density changes is available in the Supporting Information.

Both experimental and simulated data are available on the static structure factor (SSF) for PEO loaded with lithium perchlorate. The neutron-weighted static structure factor measured for deuterated $\text{P}(\text{EO})_{7.5}\text{LiClO}_4$ was reported in ref 36. Accordingly, we calculated SSF for REF electrolyte in which all hydrogen atoms were replaced by deuterium. ISAACS program³⁷ was used for structure factor calculations. In Figure 4 we compare SSF averaged over last 2 ns of REF trajectory with experimental

data.³⁶ Simulated SSF agrees well with experiment, taking into account different electrolyte composition (Table 2; PEO molecular weight and $[\text{Li}^+]/[\text{O}_{\text{PEO}}]$ ratio). It should be noted that the shoulder at ca. 0.75 \AA^{-1} related to extended-range order is correctly reproduced. In previous MD simulations with non-polarizable force field, a well pronounced peak was observed instead and was attributed to long-range order of ionic species.¹⁷ A reminiscent of this feature is observed at the very beginning of our trajectory but disappears after less than 0.05 ns of simulation (cf. inset of Figure 4); simultaneously heights of other maxima increase. On the basis of static structure factors, we can conclude that our polarizable force field reproduces correctly long-range ordering of ions and slightly overestimates order at shorter lengths.

Radial Distribution Functions and Li^+ Coordination Numbers. We start our analysis of ion complexation data from the MD trajectories with the inspection of distribution functions for selected atom pairs and Li^+ coordination numbers, because it is expectable that local environments of ions greatly influence transport properties. The last 0.5 ns of each trajectory was used to calculate radial distribution functions (RDF). The results are collected in Figure 5.

Position of the main peak for Li–O (oxygen atoms from PEO or plasticizer molecules) RDF in reference electrolyte is about 2 \AA . This agrees with the Li–O distances obtained in quantum-chemical calculations^{11,12,31} and with the results of MD simulations with a polarizable force-field for similar system (PEO + LiBF_4).¹⁶ Similar are the results for systems with acid centers. For electrolytes containing Al atoms a shoulder appears on the RDF peak at about 1.9 \AA . It is related to the Li^+ distances to the oxygen atoms adjacent to the aluminum centers and results from stronger attraction of lithium cations to these oxygen atoms because of their increased negative charge. This agrees with the results of quantum-chemical calculations predicting that Li^+ interactions with oxygen atoms at Al centers are stronger than in the case of B sites.²¹ The distance-dependent coordination number for Li–O shows that the average number of polymer oxygen atoms complexed by Li^+ ion is between 3 and 4.

The maximum of the Li–Cl RDF corresponding to Li^+ coordination to the perchlorate counterion in all electrolytes appears at about 3.7 \AA (Figure 5b). RDFs for REF and B electrolytes are similar, and values for electrolytes with Al centers are significantly smaller. Accordingly, Li–Cl coordination numbers are lower for aluminum-doped systems. Whereas in reference and B electrolytes the average number of perchlorate ions found within 4 \AA distance from the cation amounts to 1.3, the corresponding values for Al and Al-2 systems are about 0.6 and 1, respectively. This indicates smaller amount of ion pairs in electrolytes with aluminum centers. Data in Figure 5b correlate with the coordination numbers for $\text{Li}^+ - \text{O}_{\text{pol}}$ shown in Figure 5a, decreasing cation coordination to the counteranions in Al and Al-2 is accompanied by increasing Li^+ coordination to the polymer as the perchlorate oxygens in the cation solvation shell are being replaced by PEO oxygen atoms.

In Figure 5c we examine distribution of perchlorate anions near the Lewis acid center. For both kinds of centers anion interaction with the center is noticeable. A broad maximum at about 4 \AA appears in the RDF for B–Cl pairs; peak for aluminum systems is sharper and positioned at smaller distances (3.5 \AA). Data shown in Figure 5, panels b and c, suggest that anion interaction with Al center is stronger than with B atom, the effect is more pronounced for aluminum centers in plasticizer molecules.

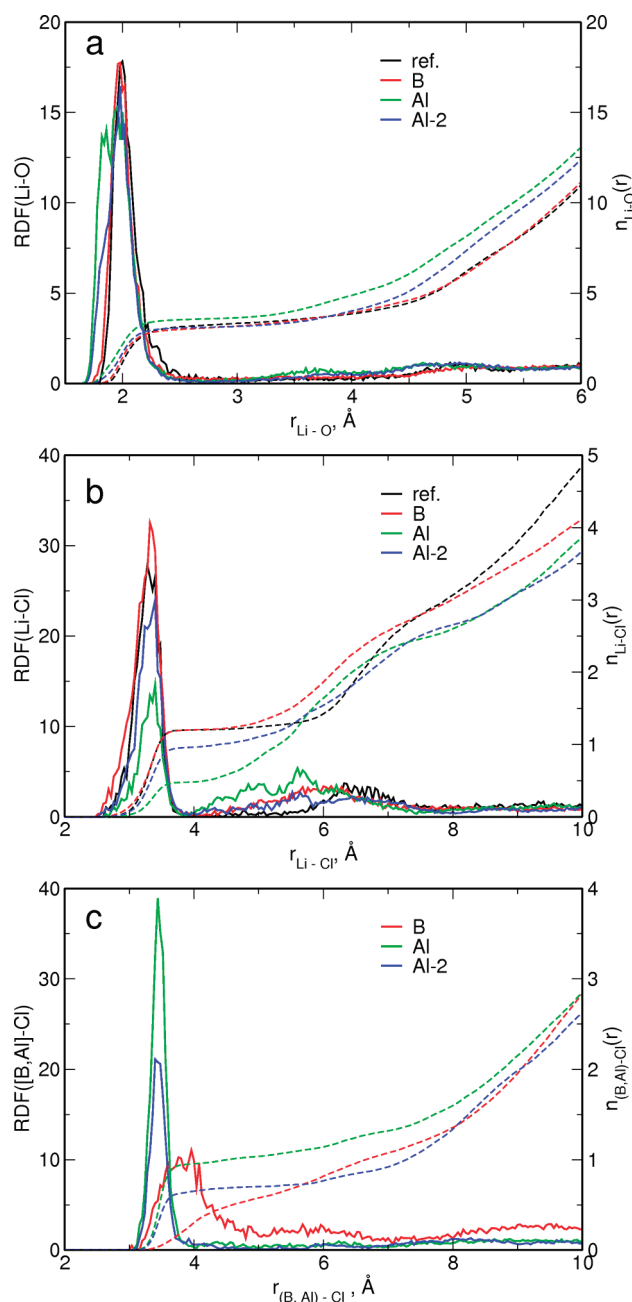


Figure 5. Radial distribution functions and distance-dependent coordination numbers for $\text{Li}^+ - \text{O}_{\text{pol}}$ (a), $\text{Li}^+ - \text{Cl}$ (b), and acid center-Cl (c) pairs.

To gain more insight into the details of the Li^+ environment, we present in Figure 6 the probability of finding given number of oxygen atoms within the 3 Å distance from the cation. In addition to polymer-like oxygens from PEO chain or plasticizer molecules (O_{pol}) we include in analysis also the oxygen atoms from perchlorate anions (O_{perch}). As readily seen, Li^+ cation in the reference electrolyte is coordinated to 3–4 polymer oxygens and 1–2 oxygen atoms from the anion, which results in the overall (including both types of oxygen atoms) coordination number is similar to that reported for MD simulations with nonpolarizable force field.¹⁷ On the other hand the average number of O_{pol} atoms around the ion is higher and the number

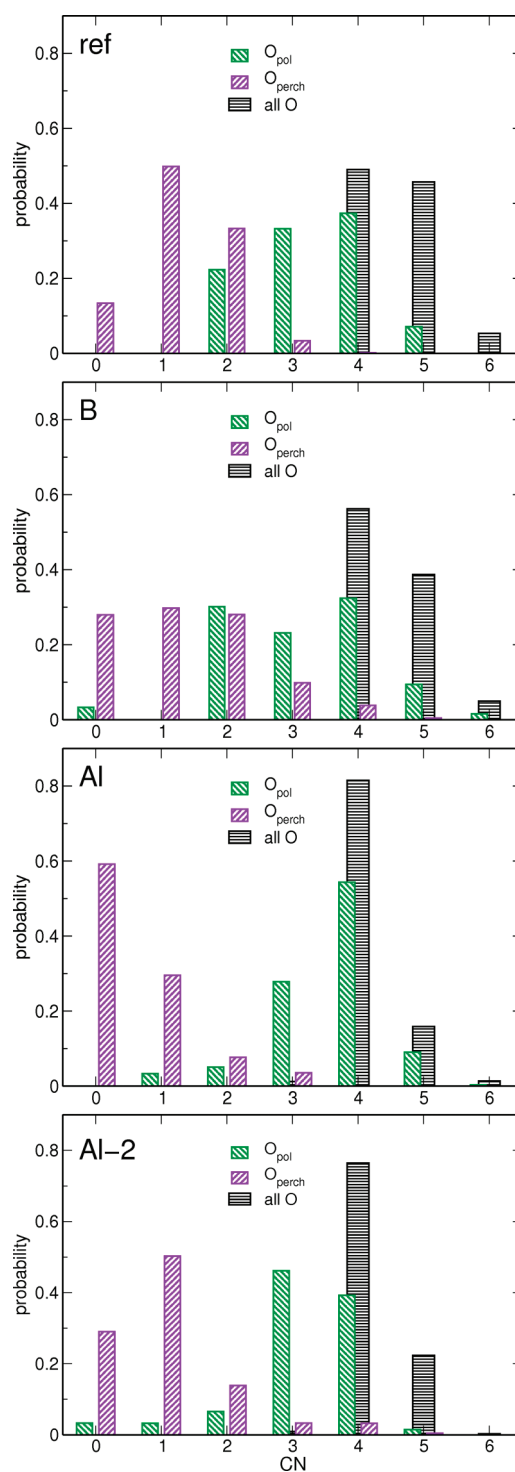


Figure 6. Distributions of $\text{Li}^+ - \text{O}$ coordination numbers. Polymer-like oxygens and oxygen atoms from perchlorate anions are distinguished.

of O_{perch} oxygens is lower than in ref 17, which shows that the polarizable force field yields better agreement with experimental neutron diffraction data suggesting that 4–5 oxygen atoms coordinating the Li^+ ion are predominantly PEO oxygens.³⁶ Likewise, inclusion of polarization effects leads to smaller degree of ion pairing compared to classical force field.^{17,18}

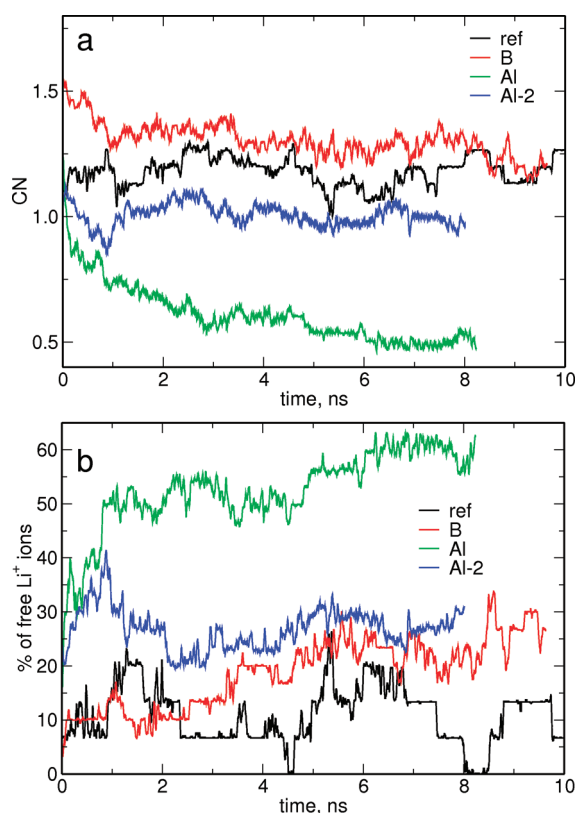


Figure 7. Average Li⁺–Cl coordination number (a) and the amount of “free” cations (b) during the MD simulation.

While experimental IR and Raman data^{38–40} and theoretical analysis of vibrational spectra^{38,40} provide evidence that there is ion pairing in PEO-based electrolytes with LiClO₄, some uncertainty about the CN of the Li⁺ ion remains. There are indications of bidentate coordination of the cation (CN = 2),³⁸ but neutron experiments³⁶ suggest rather weak Li⁺–perchlorate complexation. This feature, however, should depend on salt concentration. Indeed, analysis of Raman spectrum for P(EO)₃–LiClO₄ assigned vibrational band to the anion in C_{2v} symmetry (i.e., bidentate coordination) but the C_{3v} symmetry was postulated for P(EO)₆–LiClO₄.³⁹ Likewise, recent analysis of the solid state NMR spectra for PEO/perchlorate systems⁴¹ led to the conclusion that in P(EO)₆–LiClO₄ the Li⁺ ion is coordinated to about 5 oxygen atoms from PEO backbone. All of this data suggest that increasing PEO/salt ratio decreases Li⁺–ClO₄[–] coordination and increases cation complexation by polymer oxygens, thus coordination numbers of 1 and 2 observed in our REF system for Li⁺ interactions with perchlorate oxygen atoms are in reasonable agreement with experimental data.

In the systems with acid centers distribution of Li–O_{perch} coordination numbers shifts to lower values. Such change is the most prominent for the system with aluminate plasticizer, for which also there is an increase in probability of Li⁺ being coordinated to four O_{pol} atoms.

Our primary interest was to check how the Lewis acid centers influence the amount of Li–ClO₄[–] aggregates. To trace the dissociation of ion pairs through the MD trajectory we displayed in Figure 7 average Li–anion coordination number (the number of Cl atoms within the 4 Å radius from the cation) and the percent of “free” Li⁺ ions (i.e., with no Cl atoms within 4 Å

distance). The average number of anions coordinating Li⁺ cations in REF electrolyte is about 1.2–1.3 indicating that most cations are involved in ion pairs or even larger aggregates. As a consequence, average amount of free cations is low, about 10%. Introduction of Al centers into the electrolyte decreases the Li–anion coordination numbers and accordingly increases percentage of free lithium ions. This effect is more prominent for aluminum contained in small molecules, with Li–Cl CN decreased to 0.5 and about 60% of free cations. Smaller changes are observed for the system with Al incorporated into polymer molecules (Al-2), but nevertheless the amount of 30% free Li⁺ is three times larger than in the reference electrolyte.

The data for the boron-doped electrolyte may look surprising at first glimpse: the average Li–Cl coordination number is almost the same as in the reference electrolyte but the percentage of free cations is substantially increased and comparable to the Al-2 system. This may be rationalized with the help of Figure 6. In the B system the probability of the Li⁺–O_{perch} coordination number equal to zero increases, but simultaneously, the probabilities of CN equal to 3 and 4 also increase. It means that, indeed, there are more free cations, in agreement with Figure 7b, but the remaining cations are aggregated with counterions. Accordingly, in the B-system the amount of Li⁺ coordinated to 5 or 6 polymer oxygens increases (with respect to the reference electrolyte), but simultaneously some cations which have no close polymer-like oxygen (CN = 0) appear.

Ion Transport Properties. Technologically relevant transport properties such as ion self-diffusion coefficients and conductivity may be obtained in MD simulations from mean square displacements (MSD) of ions. The cation and anion diffusion coefficients were calculated from the slope of the time dependence of MSD

$$D = \lim_{t \rightarrow \infty} \frac{1}{6t} \langle |\mathbf{R}_i(t) - \mathbf{R}_i(0)|^2 \rangle \quad (1)$$

Of interest is also collective ion diffusion coefficient

$$D_{\text{coll}} = \lim_{t \rightarrow \infty} \frac{1}{6tN} \sum_{i,j} z_i z_j \langle [\mathbf{R}_i(t) - \mathbf{R}_i(0)][\mathbf{R}_j(t) - \mathbf{R}_j(0)] \rangle \quad (2)$$

describing the mean square displacement of the charge when the correlations between ion movement are present. This quantity is related to the conductivity of the system, which may be expressed as⁴²

$$\lambda = \lim_{t \rightarrow \infty} \frac{e^2}{6tVk_B T} \sum_{i,j} z_i z_j \langle [\mathbf{R}_i(t) - \mathbf{R}_i(0)][\mathbf{R}_j(t) - \mathbf{R}_j(0)] \rangle \quad (3)$$

In the above formulas t is time, N is the number of ions in the system, V is the volume of the simulation box, k_B is the Boltzmann’s constant, T is the temperature, e is elementary charge, z_i and z_j are the charges of ions i and j , $\mathbf{R}_i(t)$ is the position of i th ion at time t , and the brackets $\langle \rangle$ denote the ensemble average.

Mean square displacements for Li⁺ and ClO₄[–] ions in investigated systems are displayed in Figure 8a. As readily seen, ion mobility in the system with boron centers significantly increases with respect to the reference electrolyte. Conversely, ion diffusion is slower in electrolytes with aluminum sites. Diffusion enhancement in the B system is most likely an effect of viscosity decrease resulting from dilution of the polymer

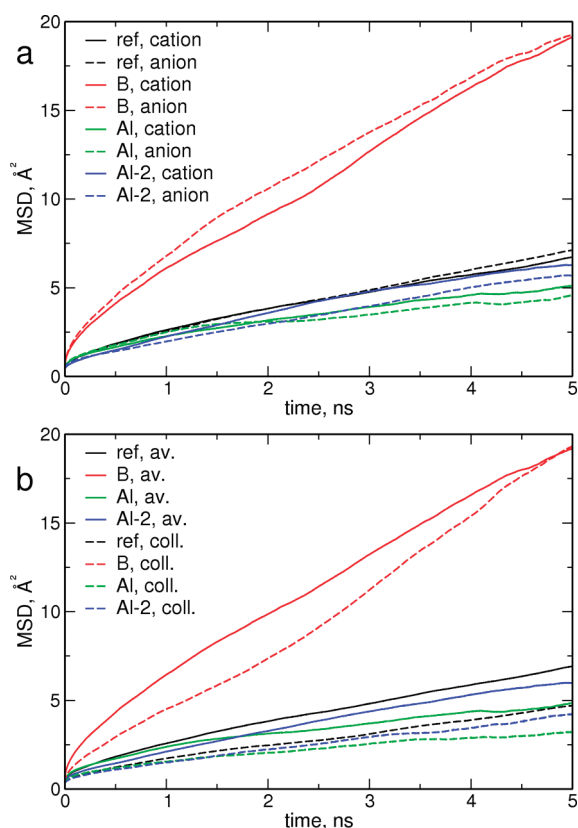


Figure 8. Mean square displacements (a) and average and collective mean square displacements (b) of ions.

matrix by small plasticizer molecules. In the systems with Al atoms anion trapping at aluminum sites, but also strong Li^+ interactions with oxygen atoms adjacent to the acid center reduce the ion mobility. Ion–Al site interactions help to understand why the ion mobility in the Al-2 electrolyte is larger than in the Al system, despite the fact that the latter contains small molecules which should facilitate ion transport. Apparently, the limiting factor in aluminum-doped systems is not the viscosity, but the strength of ion–acid center interactions. As the ions may easier approach the Al center in small plasticizer molecules, whereas it is more difficult when the Al site is bundled in the polymer chain, the interactions with the center in Al systems are stronger than in Al-2.

It may be noted that in the reference electrolyte as well as in the B system diffusion coefficients for anion are larger than for Li^+ cations. Situation changes in Al and Al-2 systems where cations move faster than perchlorate anions.

Diffusion coefficients and the apparent ion transference numbers calculated as

$$t_+ = \frac{D_+}{D_+ + D_-}, \quad t_- = 1 - t_+ \quad (4)$$

are collected in Table 3. Numerical values of D_+ and D_- confirm the above-described observations regarding relative speed of ion movements in different systems. Decreasing anion mobility in aluminum-doped systems results in cation transference numbers exceeding 0.5, whereas in reference electrolyte and B system both types of ions contribute almost equally to the charge transport (with anions slightly prevailing).

Table 3. Diffusion Coefficients, Transference Numbers, and Conductivities Obtained from the MD Data

electrolyte	D_+ [$10^{-12} \text{ m}^2/\text{s}$]	D_- [$10^{-12} \text{ m}^2/\text{s}$]	t_+	t_-	λ [10^{-3} S/m]
ref	1.7	1.9	0.48	0.52	10
B	5.7	5.7	0.49	0.51	38
Al	1.3	1.0	0.57	0.43	4.9
Al-2	1.9	1.7	0.53	0.47	8.1

In the infinitely diluted system, i.e., when no correlations between ion movements exist, conductivity may be simply related to the cation and anion diffusion coefficients. However, at larger salt concentration interactions between ions become important and lead to conductivity decrease compared to the system with independently moving ions. The measure of the amount of ion–ion correlation may be the difference between average ion diffusion coefficient $D_{\text{av}} = (D_+ + D_-)/2$ and the collective diffusion coefficient D_{coll} ; the latter quantity reduces to D_{av} when off-diagonal terms (i.e., ion–ion correlations) are negligible in eq 2. Average and collective displacements of ions are shown in Figure 8b. Collective MSD are significantly smaller than average MSD confirming strong interactions between ions in investigated electrolytes.

Conductivity values obtained from the MD data are listed in Table 3. Apparently, increase of ion diffusion in B system leads to the conductivity almost four times larger than for reference system. On the other hand, introduction of Al centers decreases the conductivity. This decrease is larger for the Al system (conductivity reaching 50% of the value for reference electrolyte). Reduced conductivity in aluminate electrolytes and the conductivity for Al-2 larger than for Al, result from ion–Al site interactions, sterically less feasible in Al-2 electrolyte as described in the above discussion of diffusion coefficients.

Conductivity of 10^{-2} S/m obtained for the reference electrolyte at 360 K is about two times larger than the value calculated at 373 K for similar system in nonpolarizable MD simulations.¹⁸ This is consistent with the findings of ref 16 that accounting for many-body polarization effects increases conductivity of the system. It is reassuring that the value of 10^{-2} S/m is of the order of conductivities measured for PEO/ LiClO_4 systems at 360–370 K.^{43,44} Measured conductivity² for PEO/ LiClO_4 system with boron acid centers at 363 K is in the range 5×10^{-2} – 10^{-1} S/m , thus our result of $4 \times 10^{-2} \text{ S/m}$ agrees well with experimental data. Likewise, the cation transference number $t_+ = 0.45$ in boron-containing electrolytes² loaded with LiClO_4 is close to our data in Table 3. We are not aware of experimental conductivity data for PEO/ LiClO_4 /aluminate systems, however, conductivities for PEO/ LiTFSI /aluminate electrolytes are of the same order as for electrolytes with boron centers.⁷ Therefore our results predicting a decrease of the conductivity in Al and Al-2 systems suggest that the force field overestimates interaction of ions with Al centers. On the other hand, part of the difference may be also attributed to different anions used in experiment and in simulations.

Interactions between Lewis acids and bases are often analyzed in terms of hard and soft acids and bases (HSAB) theory,⁴⁵ based on absolute electronegativity and absolute hardness.^{46,47} In the Supporting Information we present these parameters calculated at the B3LYP/6-311++G** level for all-trans pentaglyme, $\text{B}(\text{OCH}_2\text{CH}_2\text{OCH}_3)_3$, $\text{Al}(\text{OCH}_2\text{CH}_2\text{OCH}_3)_3$, and ClO_4^- . Electronegativity increases from pentaglyme to aluminate molecule,

showing that $\text{Al}(\text{OCH}_2\text{CH}_2\text{OCH}_3)_3$ is a stronger acid than $\text{B}(\text{OCH}_2\text{CH}_2\text{OCH}_3)_3$ and both are stronger acids than pentaerythritol. The strength of their interaction with the perchlorate anion (Lewis base) should therefore increase in the same order. This is confirmed by the calculated interaction energies ΔE . According to the HSAB theory hard acids prefer to interact with hard bases. Calculated hardnesses show that all considered molecules are hard acids, thus their effect of anion complexation is expected to be well pronounced for ClO_4^- anion being hard Lewis base. Therefore, analysis using the HSAB concept is in agreement with the results of our MD modeling of acid centers in PEO-based electrolytes.

4. CONCLUSIONS

We presented a molecular dynamics study on the effect of boron and aluminum centers in a typical polymer solid electrolyte PEO/ LiClO_4 . Combining existing force field parametrizations with supplementary quantum-chemical calculations of energies, partial atomic charges and polarizabilities we developed a suitable force field including many-body polarization.

Properties of the reference PEO/ LiClO_4 electrolyte (without Lewis acid centers) are in reasonable agreement with experimental data and available results of other MD simulations. Both radial distribution functions and coordination numbers obtained for modified electrolytes confirm interactions between boron or aluminum atoms and perchlorate anions which in turn lead to changes in local Li^+ environment. Acid centers increase the amount of cations not complexed with counterions; the effect is best pronounced for aluminum centers added in small molecules. However, presence of aluminum atoms increases also the strength of cation binding to some oxygen atoms from the polymer or plasticizer molecules, therefore reducing movements of lithium ions.

Calculated diffusion coefficients of ions and conductivities of investigated samples further corroborate conclusions about the role of acid centers. Boron atoms introduced in small plasticizer molecules increase total conductivity of the sample, but have negligible effect on Li^+ transference number. On the other hand, aluminum centers lead to significant increase of cation transference numbers, but reduce the overall conductivity. The size of this effect depends on the structure of the electrolyte (in particular, whether the aluminum atoms are added in small molecules or built into the polymer backbone) and may be related to the relative strength of ion complexation in the vicinity of acid center.

Results of molecular dynamics simulations in general support the predictions of quantum-chemical calculations regarding the anion-complexing ability of Lewis acid centers in PEO-like electrolytes. Some differences between MD simulations and experimental data (conductivity decrease in Al-enriched systems) show that further development of force field would be necessary to capture more accurately properties of PEO electrolytes with aluminum centers. Diffusion and conductivity parameters as well as data regarding average amount of free cations suggest that the technologically relevant properties of the electrolyte (transference numbers, conductivity) result from interplay of different factors (viscosity, strength of cation–anion, cation–polymer, and anion–polymer interactions, structure of the polymer) and therefore are difficult to be directly predicted solely from quantum-chemical investigations. Molecular dynamics remains therefore the tool necessary to check how

individual interactions and their balance are reflected in the electrolyte properties.

■ ASSOCIATED CONTENT

S Supporting Information. Parameters of the force field, fits of force-field energies to the quantum-chemical data, plot of density changes, and calculated HSAB data. This material is available free of charge via the Internet at <http://pubs.acs.org>.

■ AUTHOR INFORMATION

Corresponding Author

*Fax: +48 12 6340515. E-mail: eilmes@chemia.uj.edu.pl.

■ ACKNOWLEDGMENT

P.K. acknowledges support from the Polish Ministry of Science and Higher Education (Grant No. N N204 316137).

■ REFERENCES

- (1) Mehta, M. A.; Fujinami, T.; Inoue, S.; Matsushita, K.; Miwa, T.; Inoue, T. *Electrochim. Acta* **2000**, *45*, 1175.
- (2) Pennarun, P.-Y.; Jannasch, P. *Solid State Ion* **2005**, *176*, 1103.
- (3) Hirakimoto, T.; Nishiura, M.; Watanabe, M. *Electrochim. Acta* **2001**, *46*, 1609.
- (4) Kato, Y.; Hasumi, K.; Yokoyama, S.; Yabe, T.; Ikuta, H.; Uchimoto, Y.; Wakihara, M. *Solid State Ion* **2002**, *150*, 355.
- (5) Saito, M.; Ikuta, H.; Uchimoto, Y.; Wakihara, M.; Yokoyama, S.; Yabe, T.; Yamamoto, M. *J. Phys. Chem. B* **2003**, *107*, 11608.
- (6) Masuda, Y.; Nakayama, M.; Wakihara, M. *Solid State Ion* **2007**, *178*, 981.
- (7) Masuda, Y.; Seki, M.; Nakayama, M.; Wakihara, M.; Mita, H. *Solid State Ion* **2006**, *177*, 843.
- (8) Gejji, S. P.; Johansson, P.; Tegenfeldt, J.; Lindgren, J. *Comput. Polym. Sci.* **1995**, *5*, 99.
- (9) Johansson, P.; Gejji, S. P.; Tegenfeldt, J.; Lindgren, J. *Solid State Ion* **1996**, *86–88*, 297.
- (10) Sutjianto, A.; Curtiss, L. A. *J. Phys. Chem. A* **1998**, *102*, 968.
- (11) Johansson, P.; Tegenfeldt, J.; Lindgren, J. *Polymer* **1999**, *40*, 4399.
- (12) Baboul, A. G.; Redfern, P. C.; Sutjianto, A.; Curtiss, L. A. *J. Am. Chem. Soc.* **1999**, *121*, 7220.
- (13) Redfern, P. C.; Curtiss, L. A. *J. Power Sources* **2002**, *110*, 401.
- (14) Borodin, O.; Smith, G. D. *J. Phys. Chem. B* **2003**, *107*, 6801.
- (15) Halley, J. W.; Duan, Y.; Curtiss, L. A.; Baboul, A. G. *J. Chem. Phys.* **1999**, *111*, 3302.
- (16) Borodin, O.; Smith, G. D.; Douglas, R. J. *J. Phys. Chem. B* **2003**, *107*, 6824.
- (17) Siqueira, L. J. A.; Ribeiro, M. C. C. *J. Chem. Phys.* **2005**, *122*, 194911.
- (18) Siqueira, L. J. A.; Ribeiro, M. C. C. *J. Chem. Phys.* **2006**, *125*, 214903.
- (19) Borodin, O.; Smith, G. D. *J. Phys. Chem. B* **2006**, *110*, 6293.
- (20) Johansson, P.; Jacobsson, P. *Electrochim. Acta* **2005**, *50*, 3782.
- (21) Eilmes, A.; Kubisiak, P. *J. Phys. Chem. A* **2007**, *111*, 6388.
- (22) Eilmes, A.; Kubisiak, P. *Electrochim. Acta* **2011**, *56*, 3219.
- (23) Eilmes, A.; Kubisiak, P. *Solid State Ion* **2009**, *180*, 934.
- (24) Frisch, M. J.; Trucks, G. W.; Schlegel, H. B.; Scuseria, G. E.; Robb, M. A.; Cheeseman, J. R.; Scalmani, G.; Barone, V.; Mennucci, B.; Petersson, G. A.; Nakatsuji, H.; Caricato, M.; Li, X.; Hratchian, H. P.; Izmaylov, A. F.; Bloino, J.; Zheng, G.; Sonnenberg, J. L.; Hada, M.; Ehara, M.; Toyota, K.; Fukuda, R.; Hasegawa, J.; Ishida, M.; Nakajima, T.; Honda, Y.; Kitao, O.; Nakai, H.; Vreven, T.; Montgomery, Jr., J. A.; Peralta, J. E.; Ogliaro, F.; Bearpark, M.; Heyd, J. J.; Brothers, E.; Kudin, K. N.; Staroverov, V. N.; Kobayashi, R.; Normand, J.; Raghavachari, K.;

Rendell, A.; Burant, J. C.; Iyengar, S. S.; Tomasi, J.; Cossi, M.; Rega, N.; Millam, J. M.; Klene, M.; Knox, J. E.; Cross, J. B.; Bakken, V.; Adamo, C.; Jaramillo, J.; Gomperts, R.; Stratmann, R. E.; Yazyev, O.; Austin, A. J.; Cammi, R.; Pomelli, C.; Ochterski, J. W.; Martin, R. L.; Morokuma, K.; Zakrzewski, V. G.; Voth, G. A.; Salvador, P.; Dannenberg, J. J.; Dapprich, S.; Daniels, A. D.; Farkas, Ö.; Foresman, J. B.; Ortiz, J. V.; Cioslowski, J.; Fox, D. J. *Gaussian 09*, revision A.02; Gaussian, Inc.: Wallingford, CT, 2009.

(25) Cornell, W. D.; Cieplak, P.; Bayly, C. I.; Gould, I. R.; Merz, K. M., Jr.; Ferguson, D. M.; Spellmeyer, D. C.; Fox, T.; Caldwell, J. W.; Kollman, P. A. *J. Am. Chem. Soc.* **1995**, *117*, 5179.

(26) James, J. J.; Whiting, A. J. *Chem. Soc. Perkin Trans. 2* **1996**, *9*, 1861.

(27) Buckingham, R. A. *Proc. R. Soc. London A* **1938**, *168*, 264.

(28) Lennard-Jones, J. E. *Proc. R. Soc. London A* **1924**, *106*, 463.

(29) Rappe, A. K.; Casewit, C. J.; Colwell, K. S.; Goddard, W. A., III; Skiff, W. M. *J. Am. Chem. Soc.* **1992**, *114*, 10024.

(30) Ottoson, N.; Vácha, R.; Aziz, E. F.; Pokapanich, W.; Eberhardt, W.; Svensson, S.; Öhrwall, G.; Jungwirth, P.; Björneholm, O.; Winter, B. *J. Chem. Phys.* **2009**, *131*, 124706.

(31) Eilmes, A.; Kubisiak, P. *J. Phys. Chem. A* **2008**, *112*, 8852.

(32) Eilmes, A. *Chem. Phys. Lett.* **2003**, *382*, 258.

(33) Materials Studio v. 4.2, Accelrys Software, Inc.; <http://accelrys.com>.

(34) Tinker Molecular Modeling Package v. 5.0, <http://dasher.wustl.edu/tinker/>.

(35) Thole, B. T. *Chem. Phys.* **1981**, *59*, 341.

(36) Mao, G.; Saboungi, M.-L.; Price, D. L.; Baydal, Y. S.; Fischer, H. E. *Europhys. Lett.* **2001**, *54*, 347.

(37) Le Roux, S.; Petkov, V. *J. Appl. Crystallogr.* **2010**, *43*, 181.

(38) Klassen, B.; Aroca, R.; Nazri, G. A. *J. Phys. Chem.* **1996**, *100*, 9334.

(39) Ducasse, I.; Dussauze, M.; Grondin, J.; Lassègues, J.-C.; Naudin, C.; Servant, L. *Phys. Chem. Chem. Phys.* **2003**, *5*, 567.

(40) Grondin, J.; Ducasse, L.; Bruneel, J.-L.; Servant, L.; Lassègues, J.-C. *Solid. State Ion* **2004**, *166*, 441.

(41) Gao, Y.; Hu, B.; Yao, Y.; Chen, Q. *Chem.—Eur. J.* **2011**, *17*, 8941.

(42) Müller-Plathe, F. *Acta Polym.* **1994**, *45*, 259.

(43) Gorecki, W.; Andreani, R.; Berthier, C.; Armand, M.; Mali, M.; Roos, J.; Brinkmann, D. *Solid State Ion* **1986**, *18–19*, 295.

(44) Zhou, D.; Mei, X.; Ouyang, J. *J. Phys. Chem. C* **2011**, *115*, 16688.

(45) Pearson, R. G. *J. Am. Chem. Soc.* **1963**, *85*, 3533.

(46) Parr, R. G.; Pearson, R. G. *J. Am. Chem. Soc.* **1983**, *105*, 7512.

(47) Pearson, R. G. *J. Am. Chem. Soc.* **1985**, *107*, 6801.